

Analyzing Crystal Structure of Consolidated Zeolite 13X

Sujeong Lee^a, Ho Jin Ryu^{a,b,*}

^aDepartment of Materials Science and Engineering, Korea Advanced Institute of Science and Technology

^bDepartment of Nuclear and Quantum Engineering, Korea Advanced Institute of Science and Technology

*Corresponding author: hojinryu@kaist.ac.kr

1. Introduction

The usage of zeolites is wider, such as catalysis, separation, and adsorption, because of the high specific surface area with nanoporous structure, which depend on the ratio of silicon and aluminum in the framework [1]. Especially, commercial zeolite ion exchanger are used in forms such as beads, pellets, and coatings on a styrene-DVB matrix [2]. However, shaping these products requires binders and heat treatment, which can block and degrade zeolite pores. Thus, cold sintering is emerging as a substitute technique that operates at lower temperatures and without binders [3]. Shi et al. performed a study about applying cold sintering to zeolite in terms of phase identification, microstructure, and mechanical strength [4]. However, the effect of the cold sintering process on a nanoporous structure of zeolites has not been revealed but it is necessary to utilize cold sintered zeolite. Rietveld refinement is an analysis tool for the elucidation of crystal structure and atomic coordinates precisely.

Thus, in this study, the crystal structure of consolidated zeolite 13X was examined through profile matching using Fullprof, which is one of the representative Rietveld refinement software. The space group, lattice parameters, size, and strain of each consolidated zeolite 13X were calculated precisely.

2. Methods and Experiment

2.1 Materials

Zeolite 13X powder ($\text{Na}_{86}[(\text{AlO}_2)_{86}(\text{SiO}_2)_{106}] \cdot x\text{H}_2\text{O}$, 283592), sodium hydroxide (NaOH, solution, 415413) were supplied by Sigma Aldrich.

2.2 Consolidation

Four types of consolidation were used in the study as shown in Fig. 1. For sintering at 700°C, pelletized zeolite was heated up to 700°C for 4 hours. For cold sintering, there was divided into dry and wet processing. Dry cold sintering involved cold sintering only zeolite powder at 500 MPa for 10 min at 200 °C. Wet cold sintering was performed with additional liquid agents (17 wt.% of deionized water or 5 M of NaOH).



Fig. 1. Diagram of the study

2.3 Characterization

The crystal structure of consolidated zeolite X powders was investigated using X-ray diffractometry (XRD) (SmartLab, RIGAKU) with $\text{CuK}\alpha$ radiation. Data were collected in the range of $2\theta = 3\text{-}140^\circ$ with a $0.01^\circ/\text{step}$ and a scanning time was adjusted for 10,000 counts at $2\theta = 11.7^\circ$. The instrument parameters (zero-point shift, profile shape parameters) were corrected with the National Institute of Standards Technology (NIST) certified standard reference material 660b, LaB_6 , and the Thomson-Cox-Hastings pseudo-Voigt function, which is combined Lorentzian and Gaussian function, was used for the profile function in Fullprof.

3. Results and Discussion

3.1. Profile matching of each consolidated zeolite X

The crystal structure of all samples was confirmed to be face-centered cubic (space group = 203; PDF card #: 00-038-0237; sodium aluminum silicate hydrate). As shown in Fig. 2, each sample was well fitted by lattice parameters, profile shape parameters (U, V, W, X, Y), zero-point shift, displacement, and asymmetry parameters (Assym1, Assym2). The main parameters are summarized in Table 1.

Both high temperature processing and cold sintering processing did not affect the crystal phase and the lattice parameters varied in the range of 24.960-970 Å.

However, the peak broadening occurred due to different sizes and strain terms. The strain term was dominated by the Lorentzian function and the dominated size term was from the Gaussian function. Specifically, most broadening was observed in dry cold sintering samples due to the maximum strain term (0.27%) compared to other conditions. This strain term was mitigated with additional liquid agents during cold sintering.

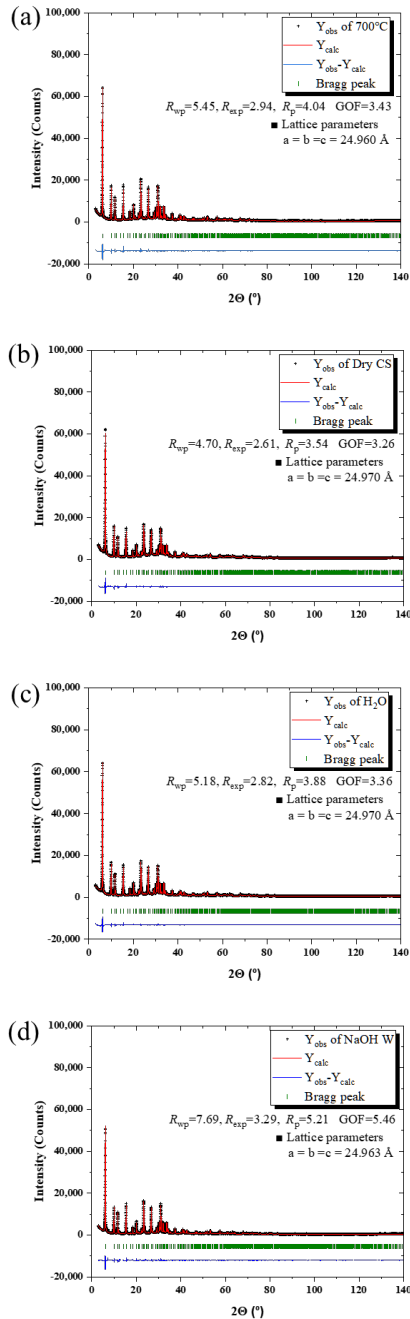


Fig. 2. Results of profile matching of all samples

Table 1. Refined parameters of all samples through Fullprof

Sample	a ($=b=c$) (Å)	X^{\dagger} (Strain)	Y^{\dagger} (Size)	U^{\dagger} (Strain)	R_w (%)	GOF^{\dagger}
REF	24.968	0.00617	0.06387	0.05604	9.45	6.72
700 °C	24.960	0.00010	0.09519	0.10026	5.47	3.62
Dry CS	24.970	0.08627	0.13846	0.25552	4.70	3.26
H ₂ O	24.970	0.00009	0.12265	0.29116	5.18	3.36
NaOH	24.963	0.00010	0.10223	0.14119	7.69	5.46

[†] where X and Y are strain and size terms of Lorentzian function; U is the strain term of Gaussian function; R_w means the weighted profile R-factor; GOF means the goodness of fit;

4. Conclusions

This study found that dry cold sintering caused the most peak broadening due to the largest strain term. However, the use of additional liquid agents mitigated the degree of peak broadening, resulting in a less ordered crystal structure than that produced by conventional heat treatment. Thus, cold sintering technique that incorporate certain liquid agents may be suitable for shaping nanoporous zeolite materials.

Acknowledgments

This study is supported by the KAI-NEET, KAIST.

REFERENCES

- [1] H. Awala *et al.*, “Template-free nanosized faujasite-type zeolites,” *Nat. Mater.* 2014 144, vol. 14, no. 4, pp. 447–451, Jan. 2015, doi: 10.1038/nmat4173.
- [2] D. H. K. W. S. I. J. W. Shin, “Removal of Radioactive Ions from Contaminated Water by Ion Exchange Resin,” *Appl. Chem. Eng.*, vol. 27, no. 6, pp. 633–638, Dec. 2016, doi: 10.14478/ACE.2016.1098.
- [3] J. Guo *et al.*, “Cold Sintering: Progress, Challenges, and Future Opportunities,” 2019, doi: 10.1146/annurev-matsci-070218.
- [4] J. Z. Shi, X. L. Zhu, L. Li, and X. M. Chen, “Zeolite ceramics with ordered microporous structure and high crystallinity prepared by cold sintering process,” *J. Am. Ceram. Soc.*, vol. 104, no. 11, pp. 5521–5528, Nov. 2021, doi: 10.1111/JACE.17964.
- [5] Z. Mu *et al.*, “Pressure-driven fusion of amorphous particles into integrated monoliths,” *Science (80-.)*, vol. 372, no. 6549, pp. 1466–1470, Jun. 2021, doi: 10.1126/science.abg1915.